Published in final edited form as:

J Immunol. 2017 February 01; 198(3): 1081–1092. doi:10.4049/jimmunol.1601307.

Autophagy in dendritic cells and B cells is critical for the inflammatory state of TLR7-mediated autoimmunity

Chi G. Weindel[1], **Lauren J. Richey**[2], **Abhiruchi J. Mehta**[3], **Mansi Shah**[3], and **Brigitte T. Huber**[1,3,*]

[1]Program in Genetics, Sackler School of Graduate Biomedical Sciences, Tufts University School of Medicine, Boston, MA, USA

[2]Division of Laboratory Animal Medicine, Tufts University, Boston, MA, USA

[3]Department of Integrative Physiology and Pathobiology, Sackler School of Graduate Biomedical Sciences, Tufts University School of Medicine, Boston, MA, USA

Abstract

Individuals suffering from autoimmune disorders possess a hyperactive cellular phenotype where tolerance to self-antigens is lost. Autophagy has been implicated in both the induction and prevention of autoimmunity, and modulators of this cellular recycling process hold high potential for the treatment of autoimmune diseases. Here we determine the effects of a loss of autophagy in dendritic cells (DCs), as well as both B cells and DCs, in a TLR7-mediated model of autoimmunity, similar to systemic lupus erythematosus, where both cell types are critical for disease. While a loss of DC autophagy slowed disease, the combined loss of autophagy in both cell types resulted in a lethal sepsis-like environment, which included tissue inflammation and hyper-production of inflammasome-associated cytokines. Ablation of B cell signaling reversed this phenotype, indicating that activation of these cells is an essential step in disease induction. Thus, autophagy plays a dichotomous role in this model of disease.

Keywords

B cells; Dendritic Cells; Systemic Lupus Erythematosus; Inflammation; Transgenic/Knockout Mice

Introduction

Inflammation is a tightly controlled biological reaction to cellular insults. An inflammatory response is required for the efficient clearance of bacterial and viral pathogens, as well as removal of cellular debris following tissue damage. Inflammation can also occur in the absence of infection. Detrimental effects of sterile inflammation are readily observed in autoimmune diseases in which inflammation is predisposed by genetic susceptibility and compounded by environmental triggers (1–4). Severe flares of inflammation mark the prototypical autoimmune disease, systemic lupus erythematosus (SLE). Inflammation in

*Correspondence to: Brigitte T. Huber; Brigitte.huber@tufts.edu; telephone: 617 636-3989.

SLE is thought to be driven by anti-nuclear Abs (ANA) as a result of a loss of self-tolerance (5).

Despite the identification of numerous SLE-susceptibility genes via genome wide association studies (GWAS), the etiology of this disease remains poorly understood (6, 7). Notably, several single nucleotide polymorphism (SNPs) associated with SLE have been mapped to autophagy-related genes (ATG) (8, 9). Targeted macroautophagy, the canonical autophagy pathway herein referred to as “autophagy”, is a key regulator of cellular homeostasis as well as immune system function; i.e., it controls recognition and clearance of extracellular pathogens (10–12), mediates cytokine production and release (13–15) and promotes the proliferation and survival of adaptive immune cells (16–19). Thus, it is reasonable to think that alterations in autophagy contribute to SLE predisposition and/or disease progression. Based on the genetic linkage and cellular functions, modulators of autophagy have an excellent potential as therapeutics for autoimmune diseases where self-tolerance has been lost (reviewed in (20, 21)). Yet, because autophagy is critical for multiple aspects of the immune system, its different functions may play opposing roles in autoimmunity. Promising results have been reported in lupus patients when treated with either inhibitors or inducers of autophagic processes (22).

To better understand the role of autophagy in SLE, we utilized a mouse model of autoimmunity, mediated by over-expression of the RNA-sensing innate immune receptor, TLR7 (*Tlr7.1* tg) (23, 24). We showed recently that B cell autophagy is required for the induction of autoimmunity (25). In particular, *Tlr7.1* tg mice harboring B cells deficient in autophagy did not make ANAs, lacked a type-I IFN signature and did not develop glomerulonephritis (25), all hallmarks of SLE.

Although B cells are central in SLE, dendritic cells (DCs) play also an important role in this disease, since they are the main producers of type-I IFNs and are essential APCs for T cell activation, both of which contribute to disease progression in humans and mouse models (26–30). Autophagy is required for IFNα production by plasmacytoid (p)DCs during viral infection (11), as well as for antigen presentation by myeloid (m)DCs (12, 31, 32). Therefore, disrupting autophagy in these cells has the potential to reduce autoimmune symptoms. Thus, we compared disease in *Tlr7.1* tg mice with either a DC-specific ablation of autophagy, or a combined loss of autophagy in DCs and B cells.

As predicted, an autophagy KO in DCs slowed disease progression and reduced IFNα production; however, *Tlr7.1* tg mice lacking autophagy in both cell types developed a rapid and lethal inflammatory condition, reminiscent of sterile sepsis, suggesting that autophagy plays a dichotomous role in disease progression. The massive inflammatory response in the latter mice was not driven by ANAs, but instead, auto-Abs against cytoplasmic material, such as cardiolipin (CL), a diphosphatidylglycerol lipid found in the mitochondrial membrane (33). These data demonstrate that B cells lacking autophagy maintain the capacity to respond to some self-antigens, although unable to produce ANAs. This is further supported by the finding that inhibition of B cell activation increased survival and reduced cytokine production in these mice, similar to what was observed in *Tlr7.1* tg mice lacking B cell autophagy (25).

Materials and Methods

Mice

All mice used in this study were on a C57BL/6J (B6) background and were analyzed at either 3, 5 or 14 months of age. B6 and *Cd11c*-Cre mice (C57BL/6J-Tg(I*tgax*-cre,-EGFP)4097Ach/J) (62) mice were purchased from The Jackson Laboratories (Bar Harbor, ME). *Tlr7.1* tg mice (C57BL/6-Tg(Tlr7)1Boll) were produced at NIH and generated by recombineering the BAC clone RP23-139P21 as previously described (23). Mice were bred at Tufts University School of Medicine; Dko mice and DBko mice were generated by intercrossing *Cd11c*-Cre and Bko mice (B6.129P2(C) $Cd19^{tm1(cre)Cgn}$ $Atg5^{tm1Myok}$) (17), respectively. Bko mice were obtained from H. Virgin (Washington University St. Louis, MO), at N9, and were backcrossed at Tufts University for an additional generation. *Tlr7.1* tg mice with one copy of $Atg5^{f/+}$ were crossed with, Dko, or DBko, mice to generate experimental cohorts. *Tlr7.1* tg mice with one copy of $Atg5^{f/+}$ and one copy of *Cd19*-$Cre^{+/-}$ were bred to DBko mice to generate cohorts containing *Tlr7.1* tg DBko *Cd19*ko mice. All animals were housed, bred and studied at Tufts University School of Medicine under approved IACUC guidelines.

Flow cytometry

Single cell suspensions of spleen and LN were made in 1× phosphate-buffered saline (PBS; 0.137M NaCl, 2.7mM KCl, 5.3mM Na_2HPO_4, 1.8mM KH_2PO_4), 2% fetal bovine serum (FBS; Atlanta Biologicals, S11550), using 70-μm nylon cell strainers (Falcon, 352350). Peritoneal cells were isolated by lavage (1× PBS, 2% FBS). Cells were blocked for FCGR2B/CD32 (eBiosciences,14-0161-85) and stained with the following mouse Abs from eBiosciences: CD11c (48-0114-82), CD3 (48-0032-80), (eFluor 450), CD23 (11-0232-82), GR1/Ly6G (11-5931-82), (FITC), PDCA1 (46-3172-80), GR1/Ly6G (45-5931-80), (PerCP-Cy5.5), B220 (47-0452-82), CD11b (47-0112-82), (eFluor 780), and BD Biosciences: CD69 (551113) (PerCP-Cy5.5), CD80 (553769), CD11b (01715B), CD138 (553714), CD69 (553237), (PE), CD5 (55035), CD21 (558658), B220 (553092), (APC). Cells were analyzed using an LSRII, FACSDiva software (BD Biosciences). Secondary analysis was performed using FCS Express 4 Research Edition (De Novo Software).

Detection of auto-Abs

HEP-2 slides (MBL Bion, AN-1012) were used to determine the presence of antinuclear IgG. Sera were diluted 1:80, and slides were treated per the manufacturer's recommendations. To identify autoreactive sera, a secondary goat anti-mouse IgG FITC (Sigma, F8264) at 1:250 was used. Slides were read using a Nikon Eclipse 80i fluorescence microscope, and analyzed with NIS-Elements software (Nikon).

Multiplex immunoassay

Sera were analyzed for 17 cytokines: IL1α, IL1β, IL2, IL4, IL5, IL6, IL10, IL12 (p70), IL13, IL17A, IL18, TNFα, MCSF, GCSF, GMCSF, IFNα, and IFNγ, using eBiosciences ProcartaPlex™ Multiplex Immunoassay, Mouse Th1/Th2 Cytokine Panel (11 plex) (EPX110-20820-901), IFNα Simplex (EPX010-26027), IL1α Simplex (EPX010-20611),

IL10 Simplex (EPX010-20614), GCSF Simplex (EPX010-26034), IL17A Simplex (EPX010-26001), and MCSF Simplex (EPX010-26039), per the manufacturer's specifications. All samples were diluted 1:1 and run in duplicate on a Luminex analyzer.

Cytokine ELISA

Cytokine levels of serum IL18 were determined as follows; plates were coated with 50μl of rat anti-mouse IL18 mAb (MBL, D047-3) at 1:1000 in 1× PBS and incubated overnight (O/N) at 4°C. Plates were blocked for 1 h in 1× PBS, 1% BSA. Standards were diluted 1:1 starting at 4ng/ml (MBL, D048-3) and samples, diluted 1:4 in blocking buffer, were added to the plate and incubated O/N at 4°C. Detection Ab, 50μl of polyclonal rat anti-mouse IL18 (MBL, D048-6) was used at a 1:2000 dilution in blocking buffer, and incubated 1h at RT. Streptavidin-HRP (R&D Systems, 4800-30-06), was added at 1:1000 and incubated for 20min at RT. For detection, 50μl TMB Substrate (BD Biosciences, 555214) was added, and reactions were stopped with 50μl 2N H_2SO_4. For all cytokine ELISAs plates were read at 450nm with *SoftMax Pro* using an *EMax* (Molecular Devices).

Ig ELISA

Nunc MaxiSorp plates (eBiosciences) were coated with either 1μg/ml unlabeled goat anti-mouse IgG (1030-01), or IgM (1021-01), (Southern Biotechnology Associates). Blocking was performed with 1% BSA in borate buffer, pH8.4. Sera were serially diluted and incubated at 4°C O/N. AP-conjugated goat anti-mouse IgG (1030-04), IgM (1021-04), IgG1 (1070-04), IgG2a (1080-04), IgG2b (1090-04), IgG2c (1079-04), or IgG3 (1100-04) at 1μg/ml were used (Southern Biotechnology Associates). Standard curves were prepared with purified mouse IgG, (Santa Cruz Biotechnology, sc-2025) IgM (0101-01), IgG1 (0102-01), IgG2a (0103-01), IgG2b (0104-01), IgG2c (0122-01), or IgG3 (0105-01) (Southern Biotechnology Associates). Plates were developed with 1mg/ml AP-substrate (Sigma, S0942) in development buffer (0.05M Na_2CO_3 pH 9.5). Plates were read at 405nm with *SoftMax Pro* using an *EMax* (Molecular Devices). CL-IgG was detected with Nunc MaxiSorp plates coated with 50μl/well 0.1mg/ml CL (Avanti Polar Lipids) in 100% EtOH and incubated uncovered O/N at 4°C. The following day plates were equilibrated at RT for 30min uncovered allowing for remaining liquid to evaporate. Plates were blocked with 1XPBS 10%FBS (Atlanta Biologicals, S11550) for 1h at RT. Standard FC1 was added at 10μg/ml in 1:3 serial dilutions. Serum was added to the plate at 1:100 in 1:3 serial dilutions at 50μl/well, and incubated for 1.5hrs at RT. HRP-conjugated goat anti-mouse IgG (ThermoFisher, 62-6520) at 1:1000 was used. For detection, 50μl TMB Substrate (BD Biosciences, 555214) was added, and reactions were stopped with 50μl 2N H_2SO_4. Plates were read at 450nm with *SoftMax Pro* using an *EMax* (Molecular Devices).

Histology

Tissue were fixed with 10% neutral buffered formalin (NBF; Sigma, HT501640) and embedded in paraffin; 5-μm sections were cut and stained with hematoxylin and eosin (H&E); 2-μm kidney sections were cut and stained with periodic acid-Schiff (PAS; Rowley Biochemical, SO-429). The pathologist performed a masked evaluation of kidney sections for membrano-proliferative glomerulonephritis using the scoring system: score 1, none to focal areas of minimal segmental PAS-positive mesangial thickening; score 2, focal to

generalized mild segmental PAS-positive mesangial thickening; score 3, generalized segmental to diffuse moderate to severe PAS-positive mesangial thickening with increased glomerular cellularity; score 4, generalized diffuse severe PAS-positive mesangial thickening with increased glomerular cellularity, dilation of Bowman's space, attenuation of normally cuboidal parietal epithelium of Bowman's capsule in male mice, mild thickening of Bowman's capsule, and small numbers of tubules dilated with protein casts. Liver inflammation was given the scoring; score 0, absent to very slight focal; score 1, very slight to slight multifocal or mild focal and suppurative; score 2, mild multifocal and suppurative; score 3, moderate multifocal or mild multifocal in both parenchymal and portal areas. Liver EMH given the scoring; score 0, absent; score 1, slight foci (1–2) of minimal megakaryocyte or myeloid cells; score 2, mild multiple foci of both megakaryocytes and myeloid cells; score 3, numerous moderate foci of both megakaryocytes and myeloid cells in portal and parenchymal areas; score 4, severe multifocal expansions of both megakaryocytes and myeloid cells in portal and parenchymal areas. Lung megakaryocyte numbers were given the following scoring: score 1, megakaryocytes absent; score 2, minimal presence of megakaryocytes (1–2); score 3, moderate numbers of megakaryocytes present; score 4, numerous megakaryocytes present throughout the sectioned lung tissue. Lung inflammation was determined as either present or absent.

Statistical analysis

Graphs were generated using Prism (GraphPad). Significance for *in vivo* and *ex vivo* assays of more than two groups were determined by either one way ANOVA followed by Tukey's multiple comparisons test, or Kruskal-Wallis' test followed by Dunn's multiple comparisons test, depending on sample distribution. Significance for two groups was determined by a two-tailed Mann-Whitney U test, where appropriate. Survival curves were analyzed using a Mantel-Cox (log-rank) test. Error bars represent SEM.

Results

Loss of DC autophagy extends lifespan and reduces type-1 IFNs in TLR7-mediated SLE

To determine if a deletion of autophagy in DCs would ameliorate TLR7-mediated autoimmunity, we bred the *Tlr7.1* tg line to mice containing a *Cd11c*-Cre-mediated DC-specific conditional deletion of *Atg5* (Dko) (see materials and methods for a full list of the genotypes and abbreviations used). As can be seen in Fig. 1A, a loss of DC autophagy significantly improved the survival of *Tlr7.1* tg mice, increasing the median survival from 28 to 40 weeks. However, as these mice aged beyond 40 weeks, their health rapidly declined, leading to a precipitous death. Because DCs are major producers of IFNα, we hypothesized that the increased survival of these mice was caused by lower production of this cytokine and a reduced IFN signature. To test this, we screened sera on an array of SLE-associated inflammatory cytokines. While the *Tlr7.1* tg mice presented with a significant increase in IFNα, this was not seen in *Tlr7.1* tg Dko mice, indicating a defect in type-1 IFN production (Fig. 1B). On the other hand, IL18 and, to a lesser extent, IL1β levels were elevated in the latter mice (Fig. 1C). These two cytokines require cleavage by caspase-1 for secretion and, therefore, are dependent on inflammasome activation (34, 35). Aside from these clear differences, other SLE-associated cytokines were similarly elevated in *Tlr7.1* tg and *Tlr7.1*

tg Dko mice, including IL12p70, IL6, and IL10 (Fig. 1D); growth factors (Fig. 1E), Th1 and Th2 cytokines were also unchanged (Fig. 1F, 1G). Considering the increased survival of the *Tlr7.1* tg Dko mice, cytokine levels similar to *Tlr7.1* tg mice with working autophagy were unexpected.

Because IFNα promotes macrophage activation and infiltration, we next examined the level of tissue inflammation in these mice to determine if lower IFNα production was resulting in a functional decrease in disease progression. Similar levels of inflammation, and cellular infiltration (Fig. 1H) were present in the livers of *Tlr7.1* tg and *Tlr7.1* tg Dko mice, indicating comparable tissue inflammation in both groups. Because SLE- associated tissue damage is caused by deposition of auto-Abs against DNA and RNA, we looked for ANA in the *Tlr7.1* tg Dko mice. Staining of HEP-2 cells revealed a similar auto-Ab profile in the sera of *Tlr7.1* tg and *Tlr7.1* tg Dko mice (Fig. 1I). These data indicate that in the absence of DC autophagy B cells are still capable of producing ANA in *Tlr7.1* tg Dko mice. Similarly, spleens from both *Tlr7.1* tg and *Tlr7.1* tg Dko mice were enlarged compared to controls (Fig. S1A, S1B). Although total B cell numbers were unchanged (Fig. S1C), the percentage of Marginal Zone (MZ) B cells was depleted in both groups of *Tlr7.1* tg mice, indicating B cell activation (Fig. S1D). Consistent with this, the percentages of $CD80^+$ B cells were significantly increased in both *Tlr7.1* tg and *Tlr7.1* Dko mice (Fig. S1E).

Thus, we conclude that B cells are the primary inducers of disease in these mice and are capable of driving disease progression, while lower production of IFNα in *Tlr7.1* tg Dko mice slows disease.

Loss of DC and B cell autophagy results in severe lethality, splenomegaly and lymphadenopathy

Because survival was increased in *Tlr7.1* tg mice with a DC loss of autophagy (Dko), likely due to a reduction in IFNα levels, while B cell activation remained unchanged, we reasoned that combining a loss of DC and B cell autophagy might ablate disease completely in *Tlr7.1* tg mice. We therefore bred the *Tlr7.1* tg line to mice containing a combined DC and B cell conditional deletion of *Atg5* (DBko). Surprisingly, we observed a drastically different phenotype than predicted; most significantly, these mice succumbed to rapid death with a median survival of 20 weeks (Fig. 2A, solid line). A considerable increase in the weight of spleens (Fig. 2B, left panel) and LNs (Fig. 2B, right panel) was apparent in these mice. Aged control mice with a double autophagy ko (DBko) also developed significant increases in the weight of secondary lymphoid organs over time (Fig. 2C). The phenotype of these mice was strongly enhanced by the *Tlr7.1* tg, as the spleens of *Tlr7.1* tg DBko mice at 12 weeks of age accounted for as much as 12% of total body weight (bw), compared to only 3% in *Tlr7.1* tg mice. In addition, the spleens of *Tlr7.1* tg DBko mice showed a complete loss of architecture, enhanced myelopoiesis and erythropoiesis and an expansion of the white pulp, as well as the red pulp (Fig. 2D). The LNs of these mice had a similar expansion of cell populations than those of their *Tlr7.1* tg littermates, while their peritoneal cavity cell numbers were normal (Fig. 2E). This latter finding is likely due to the fact that a B cell loss of autophagy inhibits development of B1 cells, which are mostly found in the peritoneum (17).

The early mortality of the *Tlr7.1* tg DBko mice, combined with the increased size, weight and cellularity of their secondary lymphoid organs, suggested excessive levels of tissue inflammation in these mice. Consistent with this, the dramatic cellular expansion in the spleens and LNs consisted of myeloid cell populations; notably, increased numbers of mDCs, neutrophils, monocytes and macrophages were observed (Fig. 3A, 3B; See Fig. S2 for myeloid cell gating strategy), while *Tlr7.1* tg mice only showed a mild increase in splenic mDCs at this early time point (Fig. 3A, left plot). In addition, an increase in inflammatory markers was seen on splenic and LN cells of *Tlr7.1* tg DBko mice, including $CD80^{high}$ DCs (Fig. 3C, 3D) and $Ly6C^{high}$ monocytes (Fig. 3E, 3F).

Loss of DC and B cell autophagy promotes inflammasome activation and organ damage

The inflammatory condition of *Tlr7.1* tg mice is well described and consists of a myeloid cell expansion, liver and kidney inflammation, as well as elevated cytokines, including IFNα, TNFα, and IL6, seen between 12–24 weeks (23). To determine if the lethality and severe secondary lymphoid expansion in *Tlr7.1* tg DBko mice was due to an accelerated disease, occurring earlier and beyond that observed in *Tlr7.1* tg littermates, we determined the levels of SLE-associated cytokines in the sera of *Tlr7.1* tg and *Tlr7.1* tg DBko mice between 12–14 weeks of age, and assessed organ inflammation. As can be seen in Fig. 4, we detected a dramatically different cytokine profile in the latter mice; namely, IL18 (Fig. 4A, left panel) and IL1β (Fig. 4A, right panel) were highly elevated, far above the levels seen in *Tlr7.1* tg Dko mice (Fig. 1C). These data indicate that loss of autophagy in B cells is enhancing the cytokine phenotype observed in *Tlr7.1* tg Dko mice. Increased serum IL18 was also observed in Dko and DBko control mice, suggesting increased inflammasome activation in the absence of autophagy. Consistent with a highly inflammatory condition, TNFα was also significantly elevated in *Tlr7.1* tg DBko mice (Fig. 4B). On the other hand, IFNα was not significantly elevated (Fig. 4C). This was surprising, because *Tlr7.1* tg DBko mice showed a severe myeloid expansion at this time point. Thus, the lack of IFNα indicates that the expansion of myeloid cells was not being driven by type-1 IFNs. At this age, *Tlr7.1* tg mice with working autophagy had normal levels of IFNα, consistent with their early stage in disease progression. *Tlr7.1* tg DBko mice also had increased levels of IL12p70, IL6 and IL10 (Fig. 4D), as well as multiple T cell cytokines (Fig. 4E, & 4F). Taken together, these data suggest that *Tlr7.1* tg DBko mice develop a severe inflammatory condition, reflective of increased inflammasome activity, as well as T cell activation. Importantly, their inflammatory phenotype occurs at an earlier time-point and does not include IFNα, the signature cytokine of SLE; thus, inflammation is driven by a different mechanism than in *Tlr7.1* tg mice with working autophagy. We conclude that *Tlr7.1* tg DBko mice develop a lethal inflammatory condition that is distinct from the inflammation present in *Tlr7.1* tg mice.

The distinct cytokine profile of *Tlr7.1* tg DBko mice mirrored a condition resembling sterile sepsis, which is typically accompanied by systemic organ damage. Therefore, we surveyed multiple organs for signs of inflammation. As expected, the livers of both *Tlr7.1* tg and *Tlr7.1* tg DBko mice showed cellular infiltrates and inflammation (Fig. 5A, Table S1). Notably however, the latter developed a more widespread condition, with lymphohistiocytic and suppurative inflammation in both the portal and parenchymal areas (Fig. 5A, far right

panel). In addition to increased inflammation, the livers of *Tlr7.1* tg DBko mice showed increased extramedullary hematopoiesis (EMH), consisting of myeloid cells and megakaryocytes (Fig. 5B, Table S1).

Unlike the *Tlr7.1* tg mice that do not develop severe lung inflammation (23), 90% of the *Tlr7.1* tg DBko mice showed lung infiltrates of lymphocytes or macrophages, as well as megakaryocytes, ranging from mild to severe. In addition, a thickening of the interstitium was observed, indicative of an inflammatory state (Fig. 5C, right panel, & 5D, summary Table S1). Interestingly, 67% of aged DBko control mice also possessed a slight increase in lung inflammation due to macrophage and neutrophil infiltrates (Fig. 5C, middle left panel).

Tlr7.1 tg mice develop glomerulonephritis, a characteristic of SLE (23, 36). Thus, the inflammatory state of *Tlr7.1* tg DBko kidneys was determined. Early in disease progression the glomeruli of these mice scored more severely on a pathology index than those of *Tlr7.1* tg mice (Table 1); however, their kidneys did not worsen with age, rather, they maintained a lower pathology score, while *Tlr7.1* tg mice developed more severe kidney pathology as disease progressed (Table 1). Overall, our data demonstrate that *Tlr7.1* tg DBko mice have multiple and more widespread organ damage than *Tlr7.1* tg mice, consistent with a sterile sepsis-like inflammatory condition.

Loss of autophagy promotes B cell recognition of mitochondrial antigens in *Tlr7.1* tg mice

The elevated serum IL18 and IL1β present in the *Tlr7.1* tg DBko mice (Fig. 4A) and *Tlr7.1* tg Dko mice (Fig. 1C) indicates increased inflammasome activity. Interestingly IL18 levels in *Tlr7.1* tg DBko mice were nearly twice that of *Tlr7.1* tg Dko mice. These data combined with the increased inflammation in *Tlr7.1* tg DBko mice compared to *Tlr7.1* tg Dko mice indicated that a B cell loss of autophagy enhanced the inflammasome activation and septic condition. Because B cells lacking autophagy were unable to produce ANA in *Tlr7.1* tg mice (25), we sought to confirm this phenotype in *Tlr7.1* tg DBko mice. As expected, sera from DBko and *Tlr7.1* tg DBko mice lacked nuclear and nucleolar staining on HEP2 slides (Fig. 6A, middle left and far right panels, Table 1), unlike those of their *Tlr7.1* tg littermates (Fig. 6A, middle right panel, Table 1). However, bright staining of either cytoplasmic components or the nuclear/cellular membrane was present in the sera of the latter (Fig. 6A, far right panels, Table 1). Because the speckled cytoplasmic pattern resembled mitochondrial staining, we tested for Abs against CL, a phospholipid that is a major component of the mitochondrial inner membrane, but is exposed to the cytosol upon mitochondrial damage (37). As can be seen in Fig. 6B, anti-CL IgG was increased in *Tlr7.1* tg DBko mice.

While both *Tlr7.1* tg and *Tlr7.1* tg DBko mice had similarly elevated total serum IgM levels (Fig. 6C, left graph), the total IgG level of *Tlr7.1* tg DBko mice was significantly increased (Fig. 6C, right graph), and IgG1 accounted for the majority of IgG in these mice (Fig. 6D). On the other hand, IgG2a and IgG2b were the predominant subtypes in *Tlr7.1* tg mice (Fig. 6E), as previously reported (24, 36). The levels of IgG2c and IgG3 were similar for all mice (Fig. 6E). These data indicate that an autophagy ko in B cells prevents production of ANA, but is permissive for production of other auto-Abs. Thus, we conclude that nuclear and cytoplasmic antigens are processed by different cellular machinery.

Hyper IL18 production and lethality in *Tlr7.1* tg DBko mice is dependent on BCR function

In addition to the presence of anti-CL IgG and high IgG1, B cells were increased in the LNs of *Tlr7.1* tg DBko mice (Fig. 7A; See Fig. S3 for lymphocyte gating strategy), and these cells had higher levels of the activation marker CD80 (Fig. 7B, Fig. S2A). B cell numbers and activation was similarly increased in the spleens (Fig. 7C, & Fig. 7D). B cell subsets were also altered in these mice, with reduced numbers of follicular and marginal zone B cells (Fig. 7E, Fig. S2B). Splenic plasmablasts were increased, but plasma cell numbers remained unchanged (Fig. 7F, Fig. S2C). Although total T cell numbers were unchanged in *Tlr7.1* tg DBko mice, increased T cell activation (CD69) was seen (Fig. 7G, Fig. S2D). The increase in B cell activation was surprising, given the defects reported to be associated with a loss of B cell autophagy (19, 38).

To test whether the inflammatory condition of *Tlr7.1* tg DBko mice was due to the hyperactivation of their B cells, we created triple ko mice, combining a *Cd19* ko with the B cell and DC loss of autophagy on the *Tlr7.1* tg background, and analyzed the survival of these mice. CD19 is critical for BCR function, since its loss decreases the B cell response to antigen. As can be seen in Fig. 7H, loss of CD19 rescued *Tlr7.1* tg DBko mice from premature death. Interestingly, the survival curve of these mice was similar to that of *Tlr7.1* tg mice with a B cell loss of autophagy, where disease is prevented (25). Furthermore, aged *Tlr7.1* tg DBko *Cd19*ko mice showed a reduction in serum IL18, similar to the levels in DBko controls (Fig. 7I). These data suggest that the lethal inflammatory disease in *Tlr7.1* tg DBko mice is initiated by B cells responding to intra- or extracellular auto-antigenic stimuli and is augmented by the *Tlr7.1* tg and a loss of DC autophagy.

Discussion

Using a TLR7-mediated model of autoimmunity (*Tlr7.1* tg) (23), we have previously shown that loss of B cell autophagy prevents disease, indicating that autophagy is required for disease development (25). In this paper, we demonstrate that autophagy deficiency in DCs slowed disease progression, but resulted in secondary effects. However, when autophagy was absent in both B cells and DCs, a severe and lethal inflammatory state was induced. These results are especially interesting, given that autophagy-associated genes have confounding roles in SLE development in humans, where polymorphisms have positive disease association only in specific populations, or are dependent on other functional factors, such as IL10 (9, 39, 40). Overall, our observations suggest that autophagy may have opposing roles in the development versus progression of disease.

The importance of DC autophagy in disease progression is evident by the increased mean survival and reduced IFNα present in the sera of *Tlr7.1* tg Dko mice, slowing down TLR7-mediated autoimmune development. However, over time disease was induced in these mice, and ANA production, liver inflammation and glomerulonephritis were present at similar levels in aged mice from both groups. Because elevated type-1 IFN expression is restricted to pDCs, even in the presence of TLR7 overexpression (30), the phenotype of *Tlr7.1* tg Dko mice suggests that a loss of DC autophagy is inhibiting the function of this cell type. In support of this, the improved survival of *Tlr7.1* tg Dko mice is similar to the increased survival seen in *Tlr7* tg mice that are unable to develop pDCs due to *Tcf4* haplodeficiency

(41). These latter mice showed reduced glomerulonephritis, although ANA production persisted. It has been shown that type-1 IFN upregulates TLR7 activity through a positive feedback loop in B cells (42). The presence of ANA and B cell activation in *Tlr7.1* tg Dko mice, as well as *Tlr7* tg *Tcf4* haplodeficient mice, indicates that B cells in *Tlr7* tg mice do not require IFNα produced by pDCs for auto-Ab production.

The clearance of apoptotic and necrotic cells, as well as microbes, by macrophages is dependent on LC3-associated phagocytosis (LAP), a pathway that relies on several components of the canonical autophagy machinery, including ATG5, ATG7 and Beclin (43). It has been shown that defects in this pathway result in increased production of proinflammatory cytokines (43, 44). Additionally, mice with a LysM-cre-mediated deletion of LAP components in macrophages, monocytes, neutrophils and mDCs develop an SLE-like disease over time, which includes auto-Ab production and glomerulonephritis. Disease progression in these mice was caused by the defective degradation of phagocytized dead cells (44). In contrast, all mice in our study had functional ATG5 in macrophages, monocytes and neutrophils. Furthermore, control Dko and DBko mice never developed auto-Abs (unpublished data). These findings indicate that mDCs, pDCs and B cells are dispensable for the clearance of apoptotic debris through LAP. In addition to the clearance of apoptotic debris, LAP is also critical for TLR9-dependent IFNα production following the uptake of DNA immune complexes in pDCs (15). LAP-dependent clearance of RNA-containing complexes has not been described; nevertheless, the IFNα defect in *Tlr7.1* tg Dko mice indicates that TLR7-dependent IFNα production by pDCs may also rely on LAP.

Given the importance of autophagy for B cell activation and plasmablast development, it was surprising that the *Tlr7.1* tg DBko mice developed a severe and lethal inflammatory condition. Their pervasive inflammation in the lung, liver and kidney, as well as the increase in inflammatory cytokines and expansion of inflammatory myeloid cells, was reminiscent of a sterile systemic inflammatory response, sepsis in the absence of acute infection (reviewed in (45)). Consistent with this, the two cytokines associated with activation of the inflammasome, IL1β and IL18, were present in the sera of these mice. Interestingly, IL18 levels were more prominently elevated than IL1β, which could be due to differences in turnover or assay sensitivity. It is also possible that IL1β is produced secondarily to IL18. Notably, IL1β was undetectable in aged Dko and DBko controls (unpublished data), while levels of IL18 were significantly elevated. The fact that IL18 and IL1β levels were not increased in *Tlr7.1* tg Bko mice (25) indicates that autophagy requirements for maintaining homeostasis and survival are cell type-specific.

In addition to myeloid cell activation in *Tlr7.1* tg DBko mice, we also observed increased B and T cell activation and elevated IgG. The high serum levels of IgG1 in *Tlr7.1* tg DBko mice, compared to IgG2a and IgG2b in *Tlr7.1* tg mice, suggest that autophagy-deficient B cells respond differently to antigen than B cells with working autophagy. Furthermore, the increase in B cell activation and total B cell numbers in *Tlr7.1* tg DBko mice indicates that these cells were surviving and undergoing class switch recombination in the absence of functioning autophagy (18). While *Tlr7.1* tg DBko mice lacked ANA, they produced auto-Abs against cytoplasmic or membranous determinants, demonstrating that Abs were being

made against organelles. This was substantiated by the finding that these mice made anti-CL Abs, indicative of damaged mitochondria.

It has been shown in some cell types that mitophagy occurs through ATG5/ATG7-independent autophagy (46, 47), and the vesicular maintenance of mitochondria is complementary to the autophagy machinery (48). Therefore, the loss of *Atg5* may allow clearance of damaged mitochondria under basal conditions. Consistent with this, control mice lacking DC and B cell autophagy did not make elevated anti-CL Abs, suggesting that the steady-state maintenance of mitochondria was not perturbed. The fact that TLR7 overexpression was required for the severe inflammatory state and anti-CL Ab production indicates that excessive cellular activation and accumulated damage might exhaust the non-canonical autophagy machinery. Alternatively, cellular stressors of mitochondria could be initiated prior to apoptosis. In support of this, CL is depleted from damaged mitochondria in neurons prior to mitochondrial expulsion from cells (49); furthermore, in these cells, CL binds directly to LC3, resulting in clearance by ATG7-dependent mitophagy (33). The presence of anti-CL Abs and damaged mitochondria in *Tlr7.1* tg DBko mice is of particular interest, given that circulating mitochondrial DNA (mtDNA) is found in the plasma of trauma patients (50). Acting as a damage associated molecular pattern, mtDNA causes inflammation and is a predictor of outcome in sepsis patients (51, 52). The role of damaged mitochondria in sepsis and acute organ damage has only recently been appreciated and is poorly understood. The phenotype of *Tlr7.1* tg DBko mice suggests that autophagy plays a role in the cellular response to tissue damage, thus, providing a potential target for direct intervention.

Either B cells or DCs from *Tlr7.1* tg DBko mice could be a source of the damaged mitochondria, resulting in CL exposure to the cytoplasm. A loss of autophagy in B cells has been shown to result in ER stress, the unfolded protein response and increased cell death following activation (19). ER stress can also lead to ROS and mitochondrial damage (53); mitochondrial damage and release of mtDNA, in turn, are known inflammasome activators (54, 55). While this would suggest that autophagy-deficient B cells respond to their own damaged mitochondria, thereby augmenting the inflammatory response seen in *Tlr7.1* tg Dko mice, our findings that *Tlr7.1* tg Bko mice had normal levels of serum IgG, IL18, and IL1β, is not consistent with this hypothesis (25). Additionally, the slight but significant increase of IL18 in Dko and DBko controls suggest that the IL18 production present is a direct result of a DC-specific loss of ATG5. Therefore, *Tlr7.1* tg DBko B cells could be responding to extracellular antigen, such as the cytoplasmic components of dying DCs. It has been shown that B cells do not require autophagy for activation through the BCR in C57BL/6 *lpr/lpr* mice (56). The notable reduction of disease in *Tlr7.1* tg DBko *Cd19*ko mice, deficient in BCR function, supports this latter hypothesis. Alternatively, high levels of IL18 have been shown to result in increased antibody production in B cells, which is mitigated by a loss of CD19 (57). The decrease in IL18 levels in *Tlr7.1* tg DBko *Cd19*ko mice, similar to that of DBko and Dko controls, further illustrates the critical role of both B cell function, and IL18 in augmenting disease.

Abs against phospholipids such as CL are associated with multiple immunological disorders, including anti-phospholipid syndrome (APS), rheumatoid arthritis and scleroderma. Patients

suffering from APS share characteristics of SLE patients, i.e., hematological malignancies and pregnancy complications (58). Anti-CL Abs have also been found in SLE patients in conjunction with ANA (59, 60). How these auto-Abs develop and contribute to disease pathogenesis remains an unanswered question. B cell depletion therapy has been shown to significantly reduce the number of anti-CL Abs in SLE patients (61) and could, thus, provide a therapeutic alternative for patients with APS. Our study sheds light on potential cellular mechanisms contributing to the production of lipid auto-Abs in these diseases.

Supplementary Material

Refer to Web version on PubMed Central for supplementary material.

Acknowledgments

We are grateful to Skip Virgin for supplying the *CD19-cre/ATG5*$^{f/f}$ mice, and we would like to thank John F. Kearney and Parisa Kalantari for interesting discussions.

This work was supported in part by NIH CTSI UL1TR001064 (BTH).

Abbreviations

APS	anti-phospholipid syndrome
ANA	anti-nuclear Abs
B6	C57BL/6J
CL	cardiolipin
DCs	dendritic cells
EMH	extramedullary hematopoiesis
GWAS	genome wide association studies
LAP	LC3-associated phagocytosis
mtDNA	mitochondrial DNA
m	myeloid
p	plasmacytoid
SLE	systemic lupus erythematosus
SNPs	single nucleotide polymorphism

References

1. Costenbader KH, Gay S, Alarcon-Riquelme ME, Iaccarino L, Doria A. Genes, epigenetic regulation and environmental factors: which is the most relevant in developing autoimmune diseases? Autoimmun Rev. 2012; 11:604–609. [PubMed: 22041580]

2. Deapen D, Escalante A, Weinrib L, Horwitz D, Bachman B, Roy-Burman P, Walker A, Mack TM. A revised estimate of twin concordance in systemic lupus erythematosus. Arthritis and rheumatism. 1992; 35:311–318. [PubMed: 1536669]

3. Gateva V, Sandling JK, Hom G, Taylor KE, Chung SA, Sun X, Ortmann W, Kosoy R, Ferreira RC, Nordmark G, Gunnarsson I, Svenungsson E, Padyukov L, Sturfelt G, Jonsen A, Bengtsson AA, Rantapaa-Dahlqvist S, Baechler EC, Brown EE, Alarcon GS, Edberg JC, Ramsey-Goldman R, McGwin G Jr, Reveille JD, Vila LM, Kimberly RP, Manzi S, Petri MA, Lee A, Gregersen PK, Seldin MF, Ronnblom L, Criswell LA, Syvanen AC, Behrens TW, Graham RR. A large-scale replication study identifies TNIP1, PRDM1, JAZF1, UHRF1BP1 and IL10 as risk loci for systemic lupus erythematosus. Nat Genet. 2009; 41:1228–1233. [PubMed: 19838195]

4. Sun C, Molineros JE, Looger LL, Zhou XJ, Kim K, Okada Y, Ma J, Qi YY, Kim-Howard X, Motghare P, Bhattarai K, Adler A, Bang SY, Lee HS, Kim TH, Kang YM, Suh CH, Chung WT, Park YB, Choe JY, Shim SC, Kochi Y, Suzuki A, Kubo M, Sumida T, Yamamoto K, Lee SS, Kim YJ, Han BG, Dozmorov M, Kaufman KM, Wren JD, Harley JB, Shen N, Chua KH, Zhang H, Bae SC, Nath SK. High-density genotyping of immune-related loci identifies new SLE risk variants in individuals with Asian ancestry. Nat Genet. 2016; 48:323–330. [PubMed: 26808113]

5. Liu Z, Davidson A. Taming lupus-a new understanding of pathogenesis is leading to clinical advances. Nat Med. 2012; 18:871–882. [PubMed: 22674006]

6. Cui Y, Sheng Y, Zhang X. Genetic susceptibility to SLE: recent progress from GWAS. J Autoimmun. 2013; 41:25–33. [PubMed: 23395425]

7. Bentham J, Morris DL, Cunninghame Graham DS, Pinder CL, Tombleson P, Behrens TW, Martin J, Fairfax BP, Knight JC, Chen L, Replogle J, Syvanen AC, Ronnblom L, Graham RR, Wither JE, Rioux JD, Alarcon-Riquelme ME, Vyse TJ. Genetic association analyses implicate aberrant regulation of innate and adaptive immunity genes in the pathogenesis of systemic lupus erythematosus. Nat Genet. 2015; 47:1457–1464. [PubMed: 26502338]

8. Ciccacci C, Perricone C, Ceccarelli F, Rufini S, Di Fusco D, Alessandri C, Spinelli FR, Cipriano E, Novelli G, Valesini G, Borgiani P, Conti F. A multilocus genetic study in a cohort of Italian SLE patients confirms the association with STAT4 gene and describes a new association with HCP5 gene. PLoS One. 2014; 9:e111991. [PubMed: 25369137]

9. Zhou XJ, Lu XL, Lv JC, Yang HZ, Qin LX, Zhao MH, Su Y, Li ZG, Zhang H. Genetic association of PRDM1-ATG5 intergenic region and autophagy with systemic lupus erythematosus in a Chinese population. Ann Rheum Dis. 2011; 70:1330–1337. [PubMed: 21622776]

10. Jounai N, Takeshita F, Kobiyama K, Sawano A, Miyawaki A, Xin KQ, Ishii KJ, Kawai T, Akira S, Suzuki K, Okuda K. The Atg5 Atg12 conjugate associates with innate antiviral immune responses. Proc Natl Acad Sci U S A. 2007; 104:14050–14055. [PubMed: 17709747]

11. Lee HK, Lund JM, Ramanathan B, Mizushima N, Iwasaki A. Autophagy-dependent viral recognition by plasmacytoid dendritic cells. Science. 2007; 315:1398–1401. [PubMed: 17272685]

12. Romao S, Gasser N, Becker AC, Guhl B, Bajagic M, Vanoaica D, Ziegler U, Roesler J, Dengjel J, Reichenbach J, Munz C. Autophagy proteins stabilize pathogen-containing phagosomes for prolonged MHC II antigen processing. J Cell Biol. 2013; 203:757–766. [PubMed: 24322427]

13. Dupont N, Jiang S, Pilli M, Ornatowski W, Bhattacharya D, Deretic V. Autophagy-based unconventional secretory pathway for extracellular delivery of IL-1beta. EMBO J. 2011; 30:4701–4711. [PubMed: 22068051]

14. Harris J, Hartman M, Roche C, Zeng SG, O'Shea A, Sharp FA, Lambe EM, Creagh EM, Golenbock DT, Tschopp J, Kornfeld H, Fitzgerald KA, Lavelle EC. Autophagy controls IL-1beta secretion by targeting pro-IL-1beta for degradation. J Biol Chem. 2011; 286:9587–9597. [PubMed: 21228274]

15. Henault J, Martinez J, Riggs JM, Tian J, Mehta P, Clarke L, Sasai M, Latz E, Brinkmann MM, Iwasaki A, Coyle AJ, Kolbeck R, Green DR, Sanjuan MA. Noncanonical autophagy is required for type I interferon secretion in response to DNA-immune complexes. Immunity. 2012; 37:986–997. [PubMed: 23219390]

16. Pua HH, Dzhagalov I, Chuck M, Mizushima N, He YW. A critical role for the autophagy gene Atg5 in T cell survival and proliferation. J Exp Med. 2007; 204:25–31. [PubMed: 17190837]

17. Miller BC, Zhao Z, Stephenson LM, Cadwell K, Pua HH, Lee HK, Mizushima NN, Iwasaki A, He YW, Swat W, Virgin HWt. The autophagy gene ATG5 plays an essential role in B lymphocyte development. Autophagy. 2008; 4:309–314. [PubMed: 18188005]
18. Conway KL, Kuballa P, Khor B, Zhang M, Shi HN, Virgin HW, Xavier RJ. ATG5 regulates plasma cell differentiation. Autophagy. 2013; 9:528–537. [PubMed: 23327930]
19. Pengo N, Scolari M, Oliva L, Milan E, Mainoldi F, Raimondi A, Fagioli C, Merlini A, Mariani E, Pasqualetto E, Orfanelli U, Ponzoni M, Sitia R, Casola S, Cenci S. Plasma cells require autophagy for sustainable immunoglobulin production. Nat Immunol. 2013; 14:298–305. [PubMed: 23354484]
20. Pierdominici M, Vomero M, Barbati C, Colasanti T, Maselli A, Vacirca D, Giovannetti A, Malorni W, Ortona E. Role of autophagy in immunity and autoimmunity, with a special focus on systemic lupus erythematosus. FASEB J. 2012; 26:1400–1412. [PubMed: 22247332]
21. Gros F, Muller S. Pharmacological regulators of autophagy and their link with modulators of lupus disease. Br J Pharmacol. 2014; 171:4337–4359. [PubMed: 24902607]
22. Fernandez D, Bonilla E, Mirza N, Niland B, Perl A. Rapamycin reduces disease activity and normalizes T cell activation-induced calcium fluxing in patients with systemic lupus erythematosus. Arthritis and rheumatism. 2006; 54:2983–2988. [PubMed: 16947529]
23. Deane JA, Pisitkun P, Barrett RS, Feigenbaum L, Town T, Ward JM, Flavell RA, Bolland S. Control of toll-like receptor 7 expression is essential to restrict autoimmunity and dendritic cell proliferation. Immunity. 2007; 27:801–810. [PubMed: 17997333]
24. Walsh ER, Pisitkun P, Voynova E, Deane JA, Scott BL, Caspi RR, Bolland S. Dual signaling by innate and adaptive immune receptors is required for TLR7-induced B-cell-mediated autoimmunity. Proc Natl Acad Sci U S A. 2012; 109:16276–16281. [PubMed: 22988104]
25. Weindel CG, Richey LJ, Bolland S, Mehta AJ, Kearney JF, Huber BT. B cell autophagy mediates TLR7-dependent autoimmunity and inflammation. Autophagy. 2015; 11:1010–1024. [PubMed: 26120731]
26. Kirou KA, Gkrouzman E. Anti-interferon alpha treatment in SLE. Clin Immunol. 2013; 148:303–312. [PubMed: 23566912]
27. Becker AM, Dao KH, Han BK, Kornu R, Lakhanpal S, Mobley AB, Li QZ, Lian Y, Wu T, Reimold AM, Olsen NJ, Karp DR, Chowdhury FZ, Farrar JD, Satterthwaite AB, Mohan C, Lipsky PE, Wakeland EK, Davis LS. SLE peripheral blood B cell, T cell and myeloid cell transcriptomes display unique profiles and each subset contributes to the interferon signature. PLoS One. 2013; 8:e67003. [PubMed: 23826184]
28. Bennett L, Palucka AK, Arce E, Cantrell V, Borvak J, Banchereau J, Pascual V. Interferon and granulopoiesis signatures in systemic lupus erythematosus blood. J Exp Med. 2003; 197:711–723. [PubMed: 12642603]
29. Nickerson KM, Cullen JL, Kashgarian M, Shlomchik MJ. Exacerbated autoimmunity in the absence of TLR9 in MRL.Fas(lpr) mice depends on Ifnar1. J Immunol. 2013; 190:3889–3894. [PubMed: 23467932]
30. Buechler MB, Teal TH, Elkon KB, Hamerman JA. Cutting edge: Type I IFN drives emergency myelopoiesis and peripheral myeloid expansion during chronic TLR7 signaling. J Immunol. 2013; 190:886–891. [PubMed: 23303674]
31. Lee HK, Mattei LM, Steinberg BE, Alberts P, Lee YH, Chervonsky A, Mizushima N, Grinstein S, Iwasaki A. In vivo requirement for Atg5 in antigen presentation by dendritic cells. Immunity. 2010; 32:227–239. [PubMed: 20171125]
32. Paludan C, Schmid D, Landthaler M, Vockerodt M, Kube D, Tuschl T, Munz C. Endogenous MHC class II processing of a viral nuclear antigen after autophagy. Science. 2005; 307:593–596. [PubMed: 15591165]
33. Chu CT, Ji J, Dagda RK, Jiang JF, Tyurina YY, Kapralov AA, Tyurin VA, Yanamala N, Shrivastava IH, Mohammadyani D, Qiang Wang KZ, Zhu J, Klein-Seetharaman J, Balasubramanian K, Amoscato AA, Borisenko G, Huang Z, Gusdon AM, Cheikhi A, Steer EK, Wang R, Baty C, Watkins S, Bahar I, Bayir H, Kagan VE. Cardiolipin externalization to the outer mitochondrial membrane acts as an elimination signal for mitophagy in neuronal cells. Nat Cell Biol. 2013; 15:1197–1205. [PubMed: 24036476]

34. Keller M, Ruegg A, Werner S, Beer HD. Active caspase-1 is a regulator of unconventional protein secretion. Cell. 2008; 132:818–831. [PubMed: 18329368]
35. Srinivasula SM, Poyet JL, Razmara M, Datta P, Zhang Z, Alnemri ES. The PYRIN-CARD protein ASC is an activating adaptor for caspase-1. J Biol Chem. 2002; 277:21119–21122. [PubMed: 11967258]
36. Sun X, Wiedeman A, Agrawal N, Teal TH, Tanaka L, Hudkins KL, Alpers CE, Bolland S, Buechler MB, Hamerman JA, Ledbetter JA, Liggitt D, Elkon KB. Increased ribonuclease expression reduces inflammation and prolongs survival in TLR7 transgenic mice. J Immunol. 2013; 190:2536–2543. [PubMed: 23382559]
37. Balasubramanian K, Maeda A, Lee JS, Mohammadyani D, Dar HH, Jiang JF, St Croix CM, Watkins S, Tyurin VA, Tyurina YY, Kloditz K, Polimova A, Kapralova VI, Xiong Z, Ray P, Klein-Seetharaman J, Mallampalli RK, Bayir H, Fadeel B, Kagan VE. Dichotomous roles for externalized cardiolipin in extracellular signaling: Promotion of phagocytosis and attenuation of innate immunity. Sci Signal. 2015; 8:ra95. [PubMed: 26396268]
38. Pengo N, Cenci S. The role of autophagy in plasma cell ontogenesis. Autophagy. 2013; 9:942–944. [PubMed: 23528926]
39. Lopez P, Alonso-Perez E, Rodriguez-Carrio J, Suarez A. Influence of Atg5 mutation in SLE depends on functional IL-10 genotype. PLoS One. 2013; 8:e78756. [PubMed: 24205307]
40. Lu XL, Zhou XJ, Guo JP, Jia RL, Zhao Y, Jiang Q, Liu XY, Liu Y, Sun LY, Zhang H, Li ZG. Rs548234 polymorphism at PRDM1-ATG5 region susceptible to rheumatoid arthritis in Caucasians is not associated with rheumatoid arthritis in Chinese Han population. Chin Med J (Engl). 2011; 124:2863–2867. [PubMed: 22040493]
41. Sisirak V, Ganguly D, Lewis KL, Couillault C, Tanaka L, Bolland S, D'Agati V, Elkon KB, Reizis B. Genetic evidence for the role of plasmacytoid dendritic cells in systemic lupus erythematosus. J Exp Med. 2014; 211:1969–1976. [PubMed: 25180061]
42. Green NM, Laws A, Kiefer K, Busconi L, Kim YM, Brinkmann MM, Trail EH, Yasuda K, Christensen SR, Shlomchik MJ, Vogel S, Connor JH, Ploegh H, Eilat D, Rifkin IR, van Seventer JM, Marshak-Rothstein A. Murine B cell response to TLR7 ligands depends on an IFN-beta feedback loop. J Immunol. 2009; 183:1569–1576. [PubMed: 19587008]
43. Martinez J, Almendinger J, Oberst A, Ness R, Dillon CP, Fitzgerald P, Hengartner MO, Green DR. Microtubule-associated protein 1 light chain 3 alpha (LC3)-associated phagocytosis is required for the efficient clearance of dead cells. Proc Natl Acad Sci U S A. 2011; 108:17396–17401. [PubMed: 21969579]
44. Martinez J, Cunha LD, Park S, Yang M, Lu Q, Orchard R, Li QZ, Yan M, Janke L, Guy C, Linkermann A, Virgin HW, Green DR. Noncanonical autophagy inhibits the autoinflammatory, lupus-like response to dying cells. Nature. 2016; 533:115–119. [PubMed: 27096368]
45. Lord JM, Midwinter MJ, Chen YF, Belli A, Brohi K, Kovacs EJ, Koenderman L, Kubes P, Lilford RJ. The systemic immune response to trauma: an overview of pathophysiology and treatment. Lancet. 2014; 384:1455–1465. [PubMed: 25390327]
46. Hirota Y, Yamashita S, Kurihara Y, Jin X, Aihara M, Saigusa T, Kang D, Kanki T. Mitophagy is primarily due to alternative autophagy and requires the MAPK1 and MAPK14 signaling pathways. Autophagy. 2015; 11:332–343. [PubMed: 25831013]
47. Zhang J, Ney PA. Autophagy-dependent and -independent mechanisms of mitochondrial clearance during reticulocyte maturation. Autophagy. 2009; 5:1064–1065. [PubMed: 19713771]
48. Soubannier V, McLelland GL, Zunino R, Braschi E, Rippstein P, Fon EA, McBride HM. A vesicular transport pathway shuttles cargo from mitochondria to lysosomes. Curr Biol. 2012; 22:135–141. [PubMed: 22226745]
49. Kirkland RA, Adibhatla RM, Hatcher JF, Franklin JL. Loss of cardiolipin and mitochondria during programmed neuronal death: evidence of a role for lipid peroxidation and autophagy. Neuroscience. 2002; 115:587–602. [PubMed: 12421624]
50. Lam NY, Rainer TH, Chiu RW, Joynt GM, Lo YM. Plasma mitochondrial DNA concentrations after trauma. Clin Chem. 2004; 50:213–216. [PubMed: 14709653]

51. Zhang Q, Raoof M, Chen Y, Sumi Y, Sursal T, Junger W, Brohi K, Itagaki K, Hauser CJ. Circulating mitochondrial DAMPs cause inflammatory responses to injury. Nature. 2010; 464:104–107. [PubMed: 20203610]
52. Kung CT, Hsiao SY, Tsai TC, Su CM, Chang WN, Huang CR, Wang HC, Lin WC, Chang HW, Lin YJ, Cheng BC, Su BY, Tsai NW, Lu CH. Plasma nuclear and mitochondrial DNA levels as predictors of outcome in severe sepsis patients in the emergency room. J Transl Med. 2012; 10:130. [PubMed: 22720733]
53. Bronner DN, Abuaita BH, Chen X, Fitzgerald KA, Nunez G, He Y, Yin XM, O'Riordan MX. Endoplasmic Reticulum Stress Activates the Inflammasome via NLRP3- and Caspase-2-Driven Mitochondrial Damage. Immunity. 2015; 43:451–462. [PubMed: 26341399]
54. Zhou R, Yazdi AS, Menu P, Tschopp J. A role for mitochondria in NLRP3 inflammasome activation. Nature. 2011; 469:221–225. [PubMed: 21124315]
55. Nakahira K, Haspel JA, Rathinam VA, Lee SJ, Dolinay T, Lam HC, Englert JA, Rabinovitch M, Cernadas M, Kim HP, Fitzgerald KA, Ryter SW, Choi AM. Autophagy proteins regulate innate immune responses by inhibiting the release of mitochondrial DNA mediated by the NALP3 inflammasome. Nat Immunol. 2011; 12:222–230. [PubMed: 21151103]
56. Arnold J, Murera D, Arbogast F, Fauny JD, Muller S, Gros F. Autophagy is dispensable for B-cell development but essential for humoral autoimmune responses. Cell Death Differ. 2016; 23:853–864. [PubMed: 26586568]
57. Enoksson SL, Grasset EK, Hagglof T, Mattsson N, Kaiser Y, Gabrielsson S, McGaha TL, Scheynius A, Karlsson MC. The inflammatory cytokine IL-18 induces self-reactive innate antibody responses regulated by natural killer T cells. Proc Natl Acad Sci U S A. 2011; 108:E1399–E1407. [PubMed: 22135456]
58. Bertolaccini ML, Contento G, Lennen R, Sanna G, Blower PJ, Ma MT, Sunassee K, Girardi G. Complement inhibition by hydroxychloroquine prevents placental and fetal brain abnormalities in antiphospholipid syndrome. J Autoimmun. 2016
59. Harris EN, Gharavi AE, Tincani A, Chan JK, Englert H, Mantelli P, Allegro F, Ballestrieri G, Hughes GR. Affinity purified anti-cardiolipin and anti-DNA antibodies. J Clin Lab Immunol. 1985; 17:155–162. [PubMed: 4068029]
60. Tincani A, Meroni PL, Brucato A, Zanussi C, Allegri F, Mantelli P, Cattaneo R, Balestrieri G. Anti-phospholipid and anti-mitochondrial type M5 antibodies in systemic lupus erythematosus. Clin Exp Rheumatol. 1985; 3:321–326. [PubMed: 4085163]
61. Ioannou Y, Lambrianides A, Cambridge G, Leandro MJ, Edwards JC, Isenberg DA. B cell depletion therapy for patients with systemic lupus erythematosus results in a significant drop in anticardiolipin antibody titres. Ann Rheum Dis. 2008; 67:425–426. [PubMed: 17905784]
62. Stranges PB, Watson J, Cooper CJ, Choisy-Rossi CM, Stonebraker AC, Beighton RA, Hartig H, Sundberg JP, Servick S, Kaufmann G, Fink PJ, Chervonsky AV. Elimination of antigen-presenting cells and autoreactive T cells by Fas contributes to prevention of autoimmunity. Immunity. 2007; 26:629–641. [PubMed: 17509906]

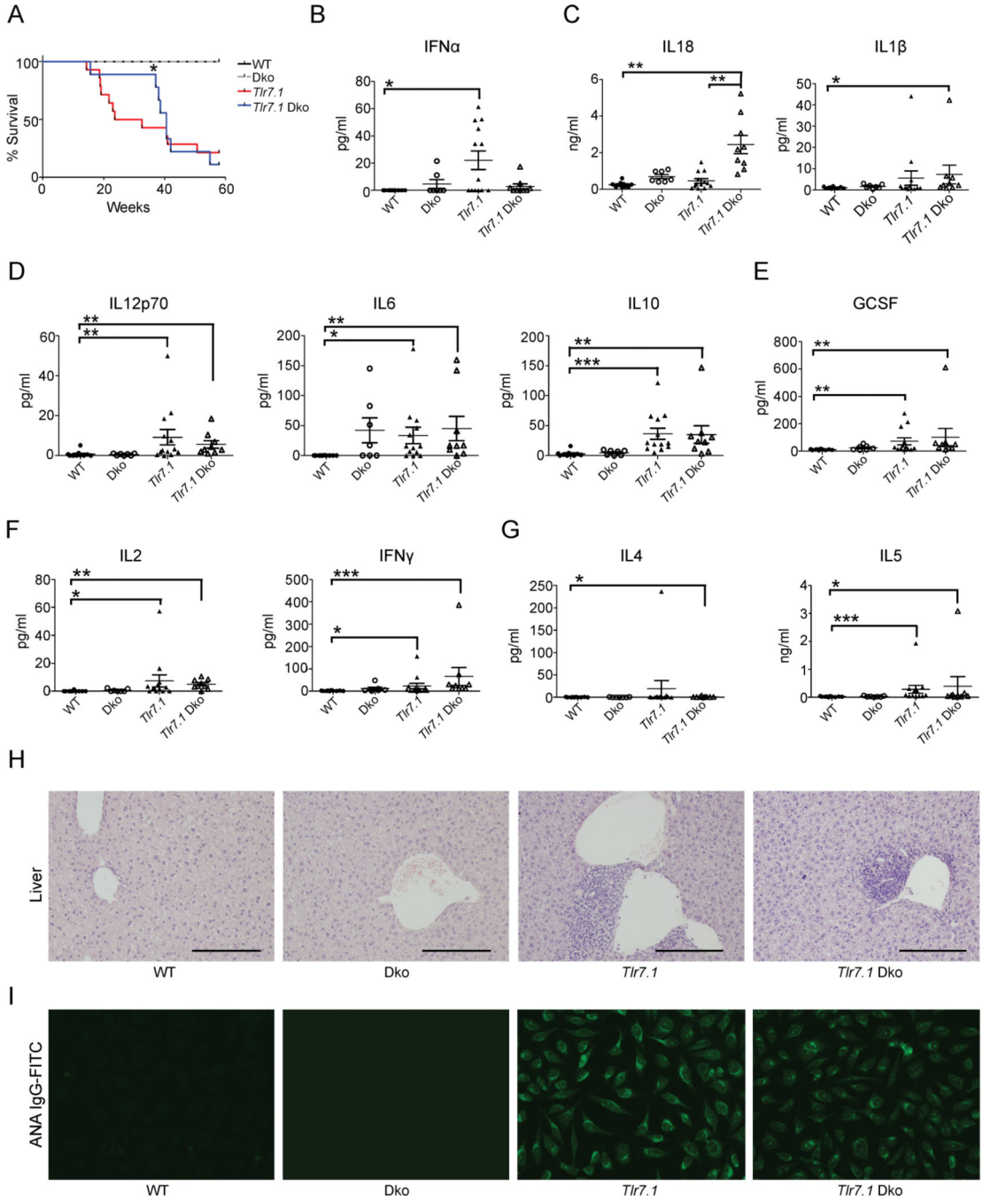

Fig 1. *Tlr7.1* tg mice lacking DC autophagy have increased lifespan and reduced IFNα

(**A**) Survival of *Tlr7.1* tg mice (red line) compared to *Tlr7.1* tg Dko mice (blue line). Mice were observed over 58 weeks. Controls (n=13), *Tlr7.1* tg (n=14), *Tlr7.1* tg Dko (n=9). (*p<0.05 Mantel-Cox log rank test). (**B–G**) Sera from age-matched non-moribund mice between 16–20 weeks of age were tested for cytokines using multiplex immunoassays: (**B**) IFNα; (**C**) IL18, and IL1β, (**D**) IL12p70, IL6, IL10, (**E**) GCSF, (**F**) IL2, IFNγ, (**G**) IL4, and IL5. Each point is representative of an individual animal. (**H**) Representative H&E sections of liver for controls (left panels), *Tlr7.1* tg (right center panel) and *Tlr7.1* tg Dko mice (far

right panel). (**I**) HEP2 slides used to detect IgG-ANA in 16–20 week old mice. Results are based on at least 6 mice per genotype (*p<0.05 **p<0.01, ***p<0.005, Kruskal-Wallis test with Dunn's post-test).

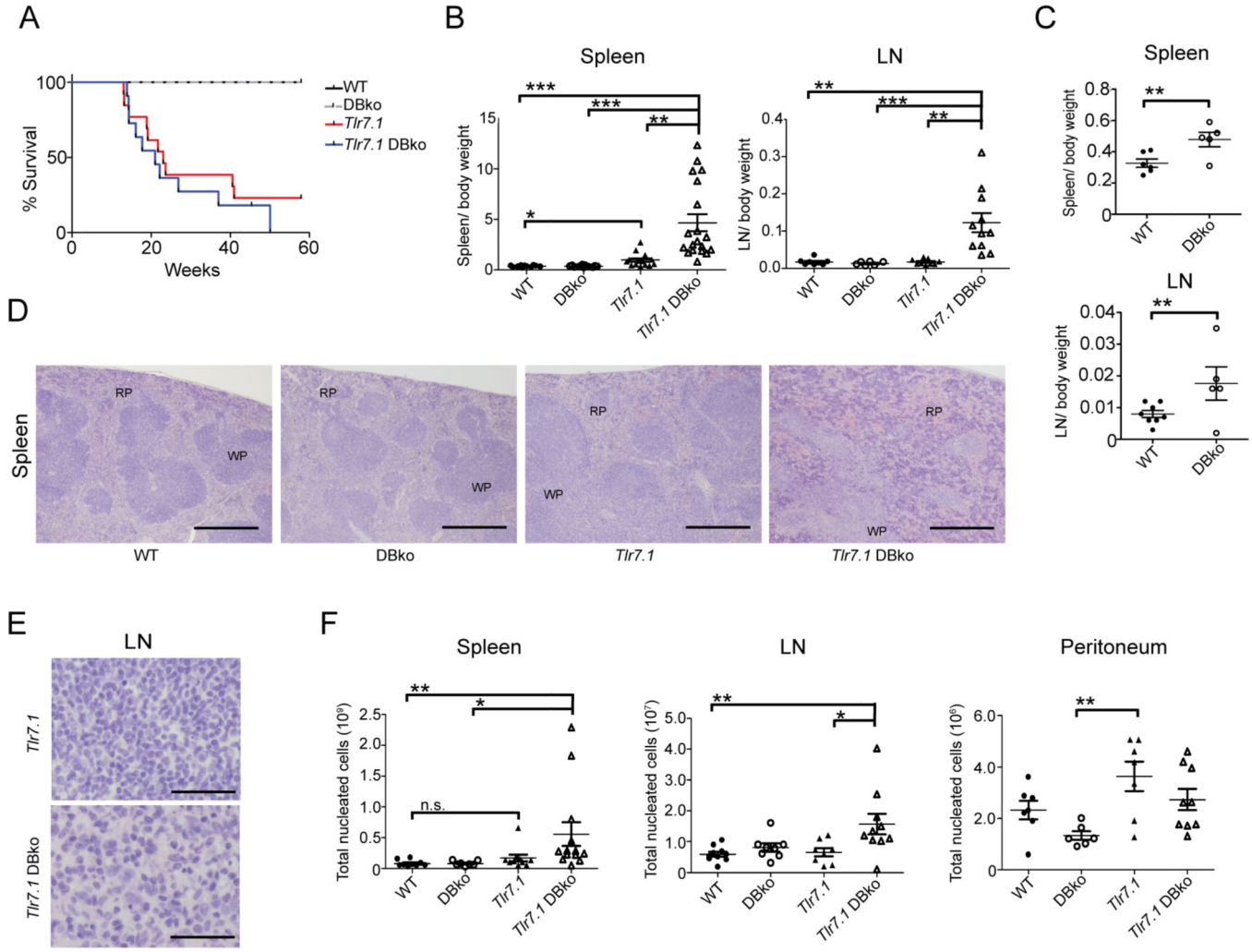

Fig 2. Loss of DC and B cell autophagy results in splenomegaly and lymphadenopathy

(**A**) Survival of *Tlr7.1* tg mice (red line) compared to *Tlr7.1* tg DBko mice (blue line). Mice were observed over 58 weeks. Controls (n=13), *Tlr7.1* tg (n=13), *Tlr7.1* tg DBko (n=11). (*p<0.05 Mantel-Cox log rank test). Spleens and LNs were weighed and normalized as a percentage of body weight at (**B**) 12–14 weeks, (**C**) and at 57 weeks for controls. Each point is representative of an individual animal. Results are based on at least 3 independent experiments. (**D & E**) H&E sections of spleen (**D**) white pulp (wp) and red pulp (rp) for controls (left panel), *Tlr7.1* tg (center panel) and *Tlr7.1* tg *Atg5*ko mice (right panel). Results are based on at least 6 mice per genotype. 40× magnification of LNs (**E**) showing nuclei, (hematoxylin - blue), and cytoplasm, (eosin - pink) for *Tlr7.1* (upper panel) and *Tlr7.1* tg *Atg5*ko (lower panel) mice. (**F**) Flow cytometry of nucleated cells for spleen (left plot), LNs (middle plot), and peritoneum (right plot). Results are based on at least 3 independent experiments with mice between 12–14 weeks of age. (*p<0.05 **p<0.01, ***p<0.005, Kruskal-Wallis test with Dunn's post-test).

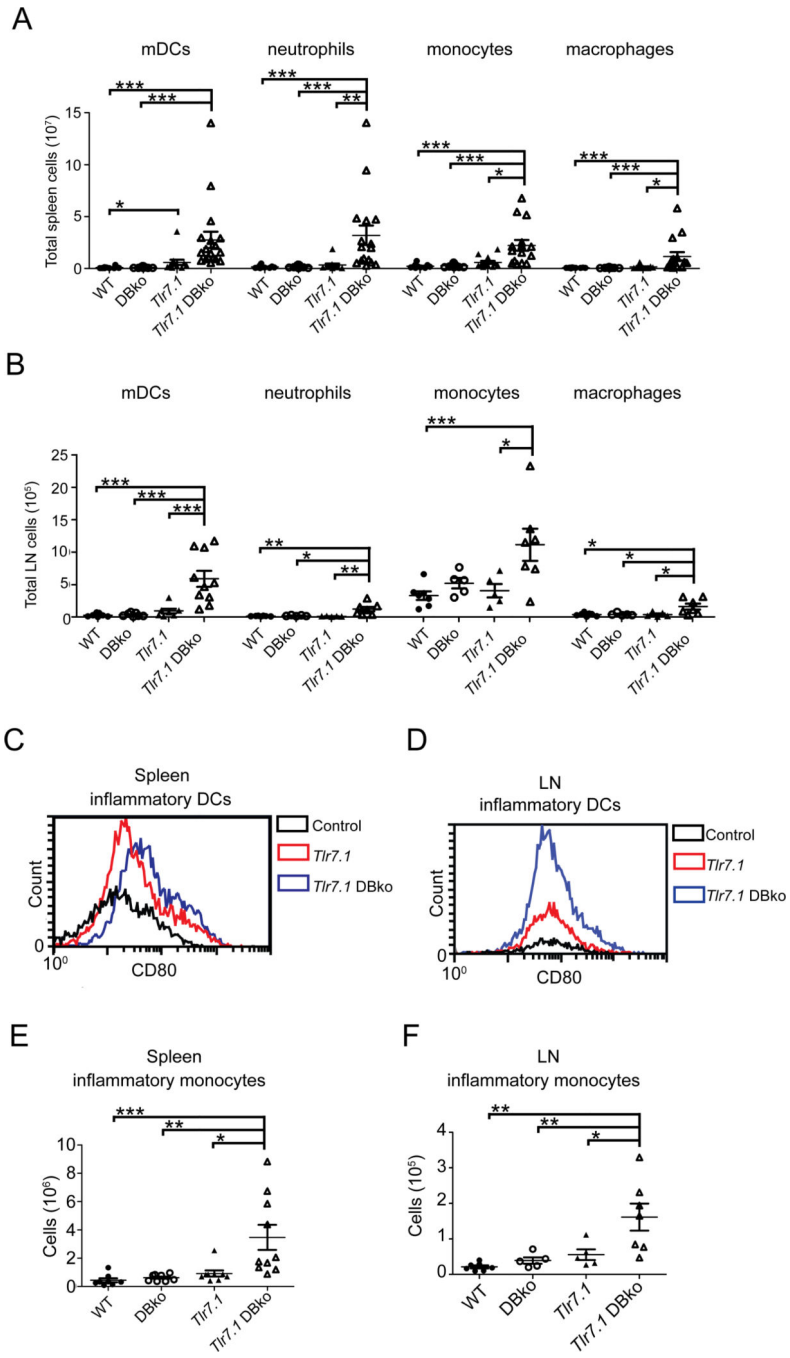

Figure 3. Loss of B cell and DC autophagy results in a systemic expansion of myeloid lineage cells in *Tlr7.1* tg mice

A. & B. Myeloid and granuloid cell populations in the spleen (**A.**), and LNs (**B.**), as well as activated DCs (**C, D.**) and inflammatory monocytes (**E, F.**) were analyzed by flow cytometry. mDCs ($CD11c^+$ $CD11b^+$ $B220^-$), monocytes ($CD11b^+$ $GR1^{low/-}$ $CD11c^-$ FSC SSC), macrophages ($CD11b^+$ $GR1^{low/-}$ $CD11c^-$ FSC SSC) neutrophils ($CD11b^+$ $GR1^+$ $CD11c^-$), activated DCs ($CD11c^+$ $B220^-$ $CD80^+$), inflammatory monocytes ($CD11b^+$

$GR1^{low/-}$ $CD11c^{-}$ $Ly6C^{high}$).). Each point is representative of an individual animal (*p<0.05 **p<0.01, ***p<0.005, Kruskal-Wallis test with Dunn's post-test).

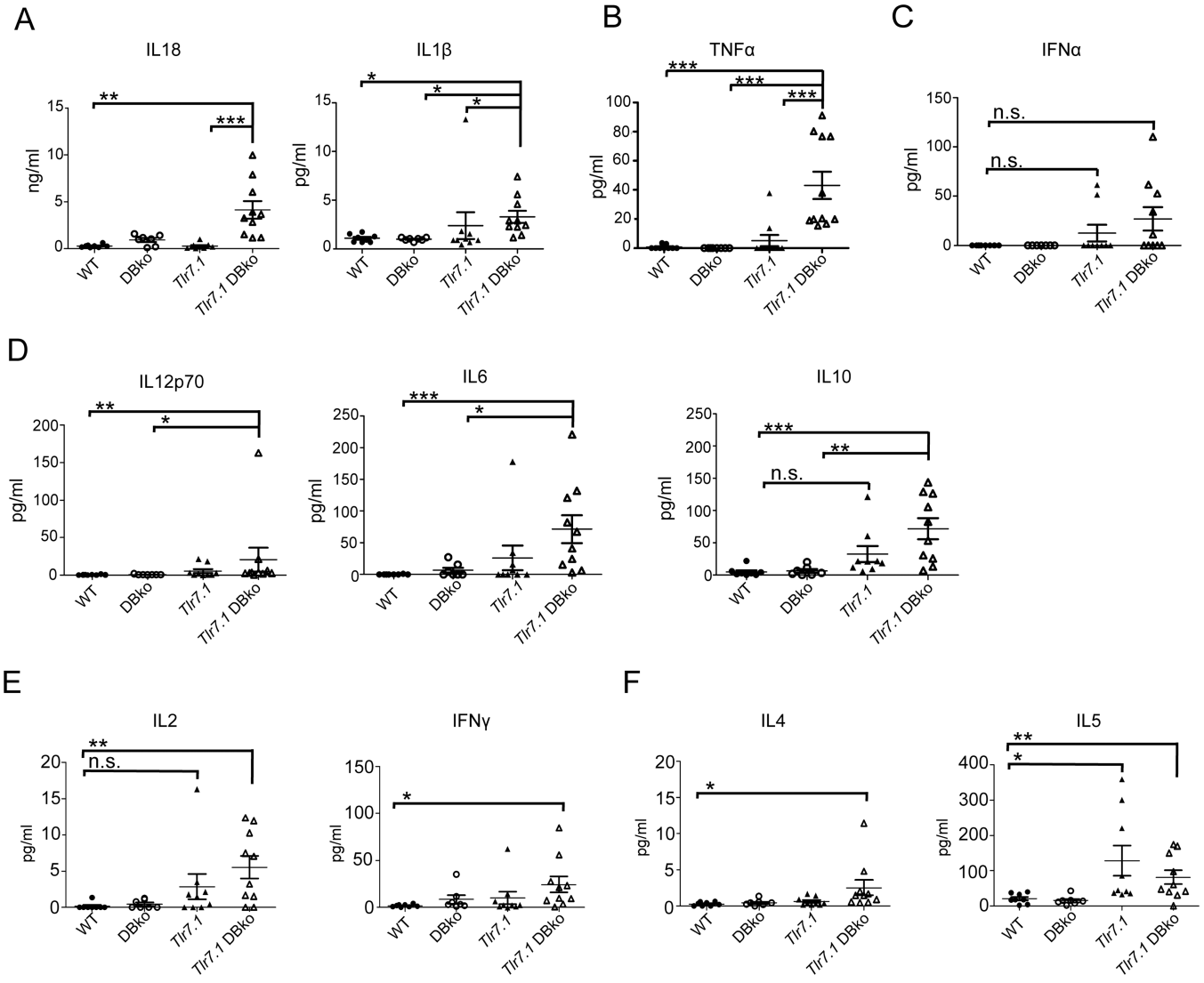

Fig 4. Inflammasome-associated cytokines are elevated upon loss of DC and B cell autophagy

Sera from age-matched non-moribund mice between 12–14 weeks of age were tested for cytokines using multiplex immunoassay. (**A**) IL-18, and IL-1β; (**B**) TNFα; (**C**) IFNα; (**D**) IL12p70, IL6, IL10; (**E**) IL2, IFNγ; **(F**) IL4, and IL5. Each point is representative of an individual animal. (*p<0.05 **p<0.01, ***p<0.005, Kruskal-Wallis test with Dunn's post-test).

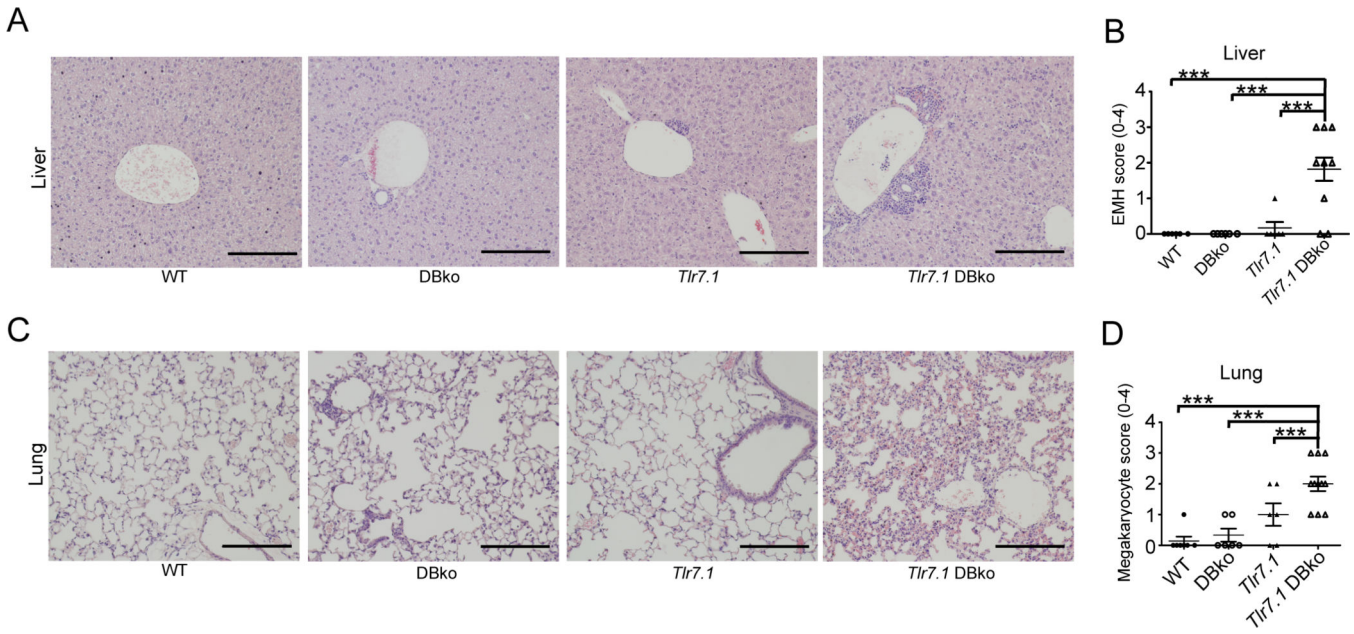

Fig 5. Multi-organ inflammation is present in *Tlr7.1* tg DBko mice

Representative H&E sections of liver (**A**) showing cellular infiltrates for WT (far left), DBko (middle left), *Tlr7.1* tg (middle right) and *Tlr7.1* tg DBko (far right) mice. WT n=(6), DBko (n=6), *Tlr7.1* tg (n=7), *Tlr7.1* tg DBko (n=10). (**B**) EMH scoring for liver sections. H&E sections of lung (**C**), showing interstitial thickening and cellular infiltrates for WT (far left), DBko (middle left), *Tlr7.1* tg (middle right) and *Tlr7.1* tg DBko (far right) mice. WT n=(6), DBko (n=6), *Tlr7.1* tg (n=7), *Tlr7.1* tg DBko (n=10). (**D**) Megakaryocyte infiltrate scoring for lung sections. Each point is representative of an individual animal with mice between 12–14 weeks of age. (*p<0.05 **p<0.01, ***p<0.005, Kruskal-Wallis test with Dunn's post-test, or one-way ANOVA with Tukey post-test where appropriate).

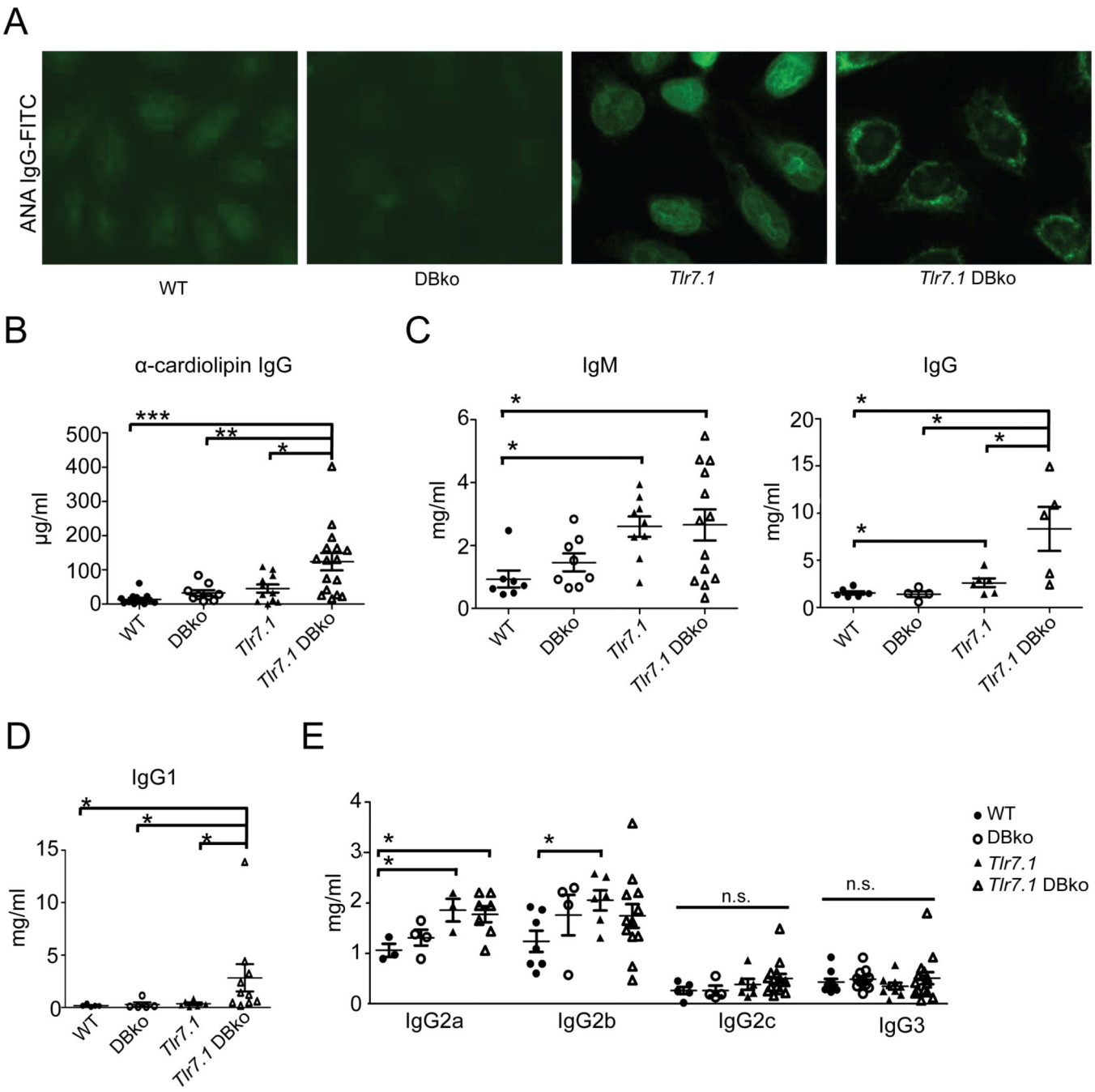

Fig 6. Auto-Abs against cardiolipin and high IgG1 are present in *Tlr7.1* tg DBko mice

(**A**) HEP2 slides used to detect IgG-ANA in 12–14 week old mice. Data are representative of 4 experiments. Controls (n=4), *Tlr7.1* tg (n=5), *Tlr7.1* tg *Atg5*ko (n=5). Antibodies against cardiolipin (**B**) total serum IgM, IgG (**C**); IgG1 (**D**); IgG2a, IgG2b, IgG2c, and IgG3 (**E**); was determined by ELISA. Each point is representative of an individual animal. Mice were between 12–14 weeks of age. (*p<0.05 **p<0.01, ***p<0.005, Kruskal-Wallis test with Dunn's post-test).

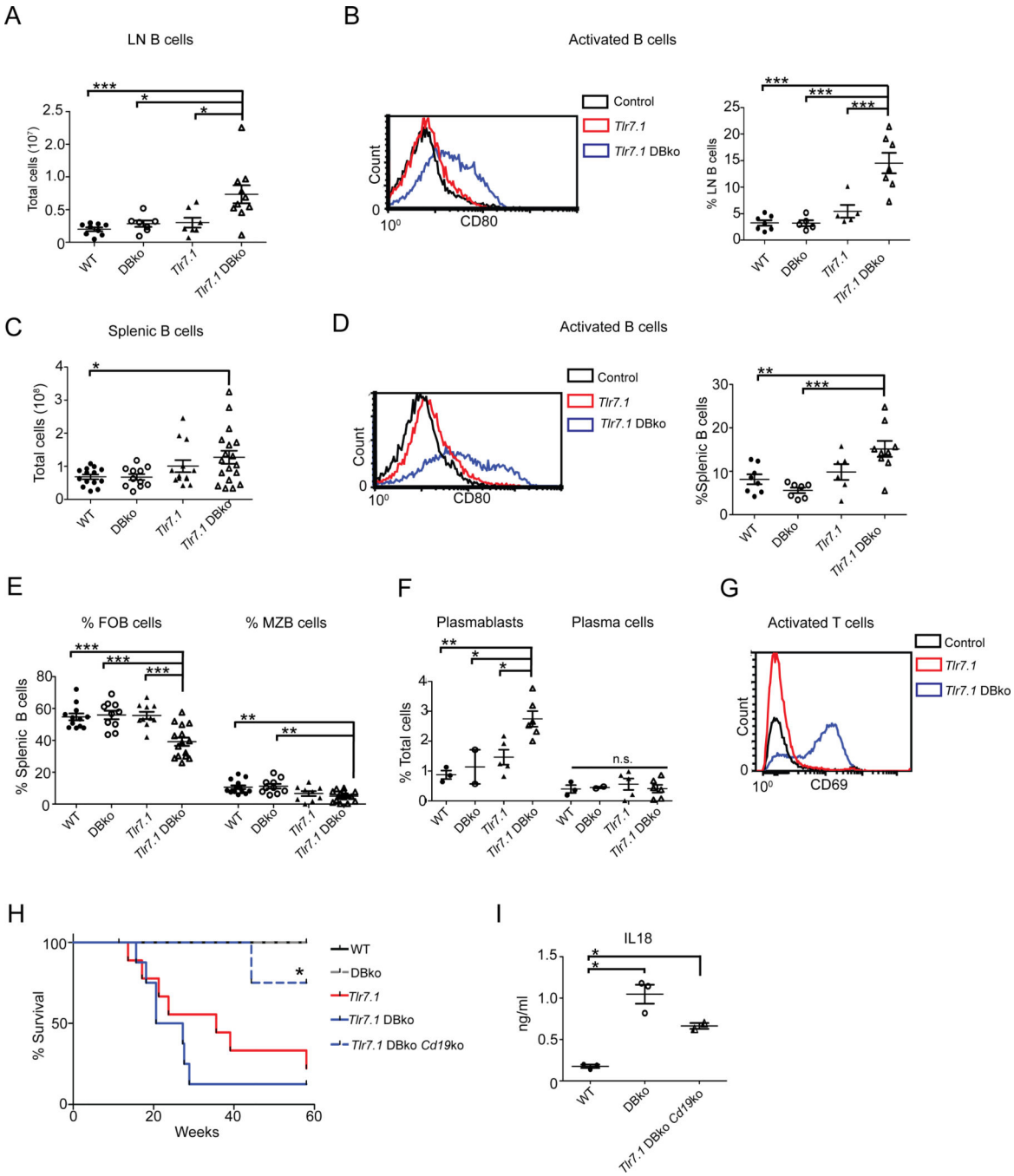

Fig 7. The sepsis-like state of *Tlr7.1* tg DBko mice is dependent on BCR activation

(**A–D**) Total LN B cell numbers, (**A**) and activation markers (B220$^+$ CD3$^-$ CD80$^+$) (**B**). Total splenic B cells (**C**) and activation markers (**D**). total B cells (B220$^+$ CD3$^-$), activated B cells (B220$^+$ CD3$^-$ CD80$^+$). (**E–G**) Splenic lymphocyte subsets (E) FO B cells, MZ B cells; (**F**) Plasmablasts and Plasma cells; (**G**) T cell activation. FO B cells (B220$^+$ CD3$^-$ CD21$^+$ CD23$^+$), MZ B cells (B220$^+$ CD3$^-$ CD21$^{low/-}$ CD23$^+$), plasmablasts (B220^{low} CD138^{mid}), and plasma cells (B220$^-$ CD138^{high}) T cell activation (B220$^-$ CD3$^+$ CD69$^+$). Each point is representative of an individual animal. Results are based on at least 3 independent

experiments with mice between 12–14 weeks of age. (**H**) Survival of *Tlr7.1* tg DBko mice (blue line) compared to *Tlr7.1* tg DBko *Cd19*ko mice (dotted blue line). Curves of mice were measured over 58 weeks. Controls (n=14), *Tlr7.1* tg (n=9), *Tlr7.1* tg DBko (n=8), *Tlr7.1* tg DBko *CD19*ko (n=5). (*p<0.05 Mantel-Cox log rank test). (**I**) ELISA for serum IL18 in mice aged 58 weeks. (*p<0.05 **p<0.01, ***p<0.005, Kruskal-Wallis test with Dunn's post-test).

Table I

Kidney pathology and ANA patterns for non-moribund and moribund mice.

	12–14 weeks			Moribund	
Kidney	**Controls**	***Tlr7.1***	***Tlr7.1* DBko**	***Tlr7.1***	***Tlr7.1* DBko**
Score	1	1.7	2.3	3.3	2.2
	12–14 weeks			**Moribund**	
ANA	**Controls**	***Tlr7.1***	***Tlr7.1* DBko**	***Tlr7.1***	***Tlr7.1* DBko**
Nuclear/nucleolar	0	2	0	3	0
Cytoplasmic	0	0	5	0	4
Mixed	0	2	0	1	0
Total	0/4	4/5	5/5	4/4	4/4